

Investigating the Morphological Categories in the NeuroMorpho Database by Using Superparamagnetic Clustering

Krissia Zawadzki¹, Mauro Miazaki¹ and Luciano da F. Costa^{1,2}

¹ Institute of Physics at Sao Carlos - University of Sao Paulo, Avenue Trabalhador Sao Carlense 400, Caixa Postal 369, CEP 13560-970, Sao Carlos, Sao Paulo, Brazil

² National Institute of Science and Technology for Complex Systems, Brazil

E-mail: krissia.zawadzki@usp.br, mauro@ursa.ifsc.usp.br, luciano@ifsc.usp.br

Abstract. The continuing neuroscience advances, catalysed by multidisciplinary collaborations between the biological, computational, physical and chemical areas, have implied in increasingly more complex approaches to understand and model the mammals nervous systems. One particularly important related issue regards the investigation of the relationship between morphology and function of neuronal cells, which requires the application of effective means for their classification, for instance by using multivariate, pattern recognition and clustering methods. The current work aims at such a study while considering a large number of neuronal cells obtained from the NeuroMorpho database, which is currently the most comprehensive such a repository. Our approach applies an unsupervised clustering technique, known as Superparamagnetic Clustering, over a set of morphological measurements regarding four major neuronal categories. In particular, we target two important problems: (i) we investigate the coherence between the obtained clusters and the original categories; and (ii) we verify for eventual subclusters inside each of these categories. We report a good agreement between the obtained clusters and the original categories, as well as the identification of a relatively complex structure of subclusters in the case of the pyramidal neuronal cells.

1. Introduction

The progress in neuroscience [1] aimed at understanding the complexity of the nervous system has continuously stimulated interdisciplinary integration between several scientific fields, such as biology, computer science [2], chemistry, and engineering. Despite the advances in these fields, there are still many remaining challenges. In this context, studies focused on morphological characterization and classification of neuronal cells have contributed substantially to enhance the neuroscientific knowledge about the relations between neuronal shape and physiology [3, 4, 5]. These discoveries are invaluable for several related areas, such as compared anatomy, neurobiology and diagnosis.

The relationship between neuronal shape and function was first suggested and investigated by Cajal [6]. Subsequently, the attention from the neuroscientists shifted to electrophysiological analysis, which focused on neuronal electrical responses to stimulus. However, evidences about morphophysiological relationships have accumulated, such as the correspondence between morphological and physiological classifications of retinal ganglion cells [7, 8]. At the same time, advances in scientific visualization and shape analysis [9] paved the way to more comprehensive and sophisticated morphological approaches, giving rise to the area of computational neuromorphometry, whose aim is to quantify and study geometrical features of neurons [10].

The onset of the free-content initiatives, such as in software, artistic works, and research papers, have motivated the creation and expansion of public databases. Indeed, a free server of data allows researchers of several fields to have immediate access to the raw materials they need in their studies. The use of these databases also facilitate the replication of experiments and results, as anyone can access the same data [11]. Another important point is the prevention of data loss, as the servers cater for backup and data maintenance.

Currently, the largest repository of neuronal cells is NeuroMorpho [12]. It contains not only the complete geometrical representation of the cells, but also several morphological measurements and data information, such as cell type, species, region, staining method, etc.

The cell categories appearing in such databases frequently take into account both morpho or eletrophysiological properties. However, there is no consensus in the classification of neurons, to the extent that reclassifications of cells have been reported periodically (e.g. [13]). The difficulties in obtaining a more definitive taxonomy are, ultimately, a consequence of the incipient situation of neuromorphological research. To begin with, there is no established set of geometrical measurements which should be used [10]. In addition, the lack of a representative number of cells allied to the choice of specific stochastic and classification methods also tends to yield varying taxonomies. Another important problem regarding the classification of neuronal cells is the identification of meaningful subcategories.

In this context, the availability of significant amounts of neurons with their

morphological properties in the NeuroMorpho repository motivated an underlying and more systematic study of classification based on morphometric features. Though several categories of neuronal cells have been traditionally adopted in the literature [3, 14, 15, 5, 10], as a consequence of the largely subjective and incomplete methods used for their definition, it is not clear how homogeneous these classes are. Therefore, the investigation of the cell distribution within each of the main classes provides a particularly important issue. Especially for the more heterogeneous cases, it is possible that the existing categories are composed of subcategories which have been overlooked as a consequence of the subjectiveness and coarseness of the previous applied measurements and classification methods. The current work sets out to investigate this important issue, namely by investigating the uniformity and possible presence of subcategories inside well-established morphological categories.

In this work, we explore the morphological measurements in NeuroMorpho by using an established classification procedure of statistical physics, known as Superparamagnetic Clustering (SPC) [16]. This method is inspired in a natural magnetic phenomenon presented by materials due to temperature variations. Described by non-homogeneous Potts model, where spins at the same state are grouped together, this physical phenomenon can be applied to data clustering applications. We used a software available in VCCLAB [17].

We chose four large categories of neurons according to the cell type-region classification and clustered them. The results were then compared to the original classification. The main objective in this work is to compare the obtained clusters with the original classification in the repository, checking the agreement between the original categories and our clustering. Since SPC is an unsupervised method, it will explore data and find clusters analysing their features without any subjective judgment. This approach can either confirm the strength of the established classification or reveal unnoticed subcategories and problems in classifications.

Our analysis presents interesting results regarding the classification of the selected categories as well as their homogeneity, leading to the necessity to investigate the possible factors which are responsible to the observed subcategories and suggesting a new classification based in the inner relations in classes that exhibits this behaviour.

This article starts by presenting the adopted database, followed by the morphological concepts relative to the measurements used in the neuronal characterization. Afterwards, the theoretical method of SPC and the software used to analyse the NeuroMorpho data are explained. Next, the results are presented and discussed.

2. Materials and Methods

2.1. NeuroMorpho Database

NeuroMorpho [18] is a contributory database containing information about digitally reconstructed neuronal cells, collected by laboratories worldwide. Publicly available,

this data is intended for researches working on issues such as studies of neuronal system complexity, visualization and neuronal modeling.

The maintenance of the database is provided by the Computational Neuroanatomy Group of the Krasnow Institute for Advanced Study, from George Mason University. This initiative is part of the Neuroscience Information Framework project [19], endorsed by the Society for Neuroscience, and includes institutes such as Cornell Univ., Yale Univ., Stanford Univ., and Univ. of California.

The database has been periodically updated. Currently, it contains data relative to 5673 neurons (version 4.0, released in 02/16/2010). We can access the original and standardized cell morphological reconstructions, as well as several data and properties such as cell type, species, brain region, animal width and weight, development age, gender, used reconstruction methods, magnification, date of upload, images of spatial structures of neurons, and references to the related literature.

In this work, we separated the data according to the cell type and brain region and selected the most numerous classes from the database. This yielded the following categories:

- Pyramidal cells from Hippocampus (Pyr-Hip);
- Medium Spiny cells from Basal Forebrain (Spi-Bas);
- Ganglion cells from Retina (Gan-Ret);
- Uniglomerular Projection neurons from Olfactory Bulb (Uni-Olf).

Table 1 presents the distribution of species within each type-region category. Since this is a public database, all data used in this article is available and easily accessible through the NeuroMorpho website. The original category names are the same as found in the database.

Table 1. Number of species in each type-region category.

Species	Spi-Bas	Pyr-Hip	Uni-Olf	Gan-Ret
Rat	232	209	0	0
Mouse	1	0	0	181
Salamander	0	0	0	64
Drosophilla	0	0	233	0

2.2. Measurements

In order to study the morphology of neurons, it is necessary to represent and characterize them in some way suitable for processing and analysis. NeuroMorpho provides L-Measure [20], a tool to extract several measurements from the neurons in the database. The measurements used in this work are illustrated in Figure 1, numbered from 1 to 19 and named as in the software documentation.

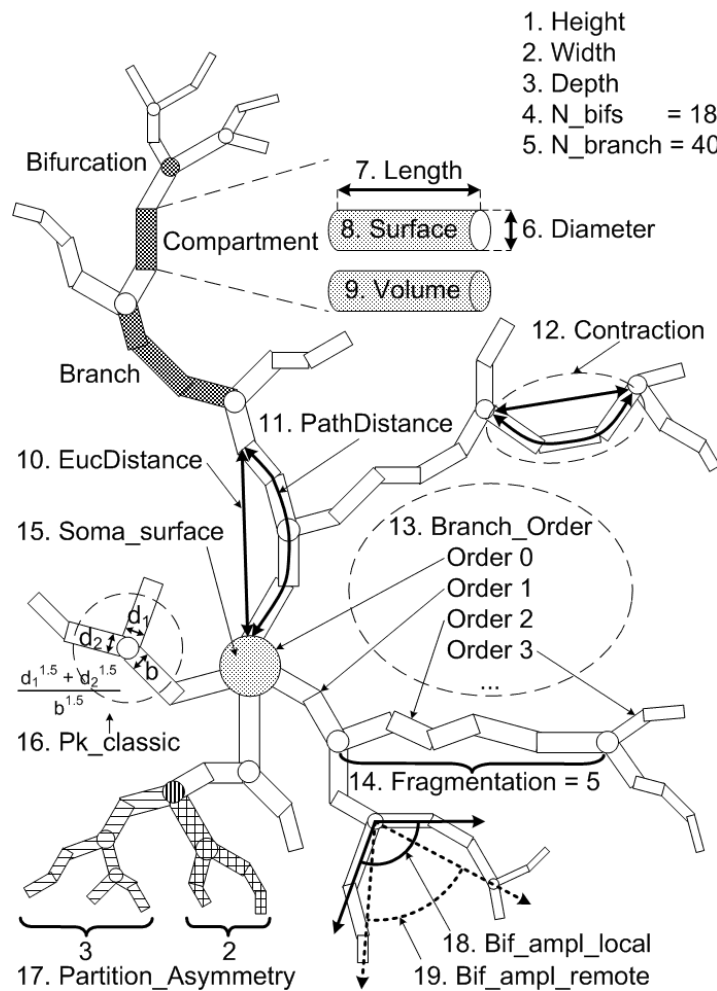


Figure 1. NeuroMorpho measurements.

The concepts of compartment, branch and bifurcation are illustrated in Figure 1. Compartments are segments represented as cylinders with diameter and extremity points coordinates. Branches are formed with one or more compartments between the soma, the bifurcations and the tips. Bifurcations are points where a branch splits into two other branches.

Measurements 1, 2 and 3 are the height, width and depth of a neuron, calculated after its alignment along the principal axis using PCA. The number of bifurcations and branches in a neuron correspond to the measurements 4 and 5. The features related to the compartment are from 6 to 9, respectively: diameter, length, surface area and volume.

The branches have their associated measurements numbered from 10 to 14. Measure 10 is the Euclidean distance between a compartment and the soma, while the path distance (11) is the sum of the lengths of the compartments between two endpoints. Contraction (12) is the ratio between the Euclidean distance and its path distance. Measure 13 is the order of the branch regarding the soma, which has order 0. The

branches attached to the soma have order 1. The branches connected to these branches have order 2, and so on. Fragmentation (14) is the number of compartments in a branch. Only compartments between bifurcations or between a bifurcation and a tip are considered.

Measurement 15 is the soma surface area. The soma can be of two types: a sphere or a set of compartments. In the latter case, the area is calculated as the sum of the area surfaces of the soma compartments.

The other measurements are related to bifurcations. Pk_classic (16) is the ratio $\frac{d_1^r + d_2^r}{b^r}$, where r is the Rall's power law value, set in this measure as 1.5, and b , d_1 and d_2 are the diameters of the bifurcation compartments (the parent and the two daughters, respectively). The partition asymmetry (17) considers the number of tips on the left and on the right daughter subtrees of a bifurcation as $n1$ and $n2$ in the expression $\frac{|n1-n2|}{n1+n2-2}$. In Figure 1, the analysed bifurcation has vertical stripes, while the left daughter subtree has horizontal stripes and the right one has a pattern of squares. Then, in this example, $n1 = 3$ and $n2 = 2$ gives $\frac{|3-2|}{3+2-2} = 0.33$. Measure 18 is the calculation of the angle between two daughter compartments in a bifurcation, while measure 19 is the angle regarding the endpoints of two daughter branches. Table 2 shows the mean values of the measurements in each category.

Table 2. Mean of the measurements in each type-region category.

Measurement	Spi-Bas	Pyr-Hip	Uni-Olf	Gan-Ret
Height	167.43	614.88	51.78	249.11
Width	182.23	576.74	117.13	247.25
Depth	66.94	353.68	56.54	21.01
N. Bifurcations	8.59	99.29	25.42	60.34
N. Branches	24.79	209.06	52.17	131.47
Diameter	0.78	0.71	1.07	0.75
Length	1266.38	23654.53	499.74	4339.40
Surface	2958.64	36941.94	1764.18	9305.34
Volume	999.01	9826.63	655.88	2455.30
Euclid. Dist.	179.08	974.86	112.58	218.86
Path Dist.	224.35	2727.95	158.07	291.82
Contraction	0.86	0.85	0.92	0.86
Branch Order	3.28	18.96	12.35	8.97
Fragmentation	1003.34	3311.95	446.99	2629.73
Soma Surface	715.14	1005.75	0.00	780.84
Pk Classic	1.30	1.60	1.77	1.62
Part. Asymmetry	0.45	0.54	0.60	0.49
Local Bif. Ampl.	63.55	69.76	93.24	82.75
Remote Bif. Ampl.	56.30	55.24	91.62	68.52

2.3. Superparamagnetic Clustering Method

The superparamagnetic method is a clustering procedure based on a physical model of a real material exhibiting magnetic response to some external parameter. Different from classical approaches, which are restricted to statistical and mathematical analysis of the system, SPC allows to evaluate how efficient is the grouping in terms of its intrinsic properties and has as additional advantages insensitivity to the initial conditions and robustness to noise. Therefore, it is necessary to understand the theoretical foundation of the physical concepts underlying the approach, and how it can be applied to data clustering.

The technique by Blatt, Wiseman and Domany [16] suggests an analogy with the generalized Ising model, also known as non-homogeneous Potts model. In this method, the temperature acts as a parameter controlling the spin configurations of a two-dimensional atoms network. It is possible to identify three reactions of the material in response to temperature variations: low, medium and high temperature intensities. They characterize the respective ferromagnetic, paramagnetic and superparamagnetic behaviour. The obtained arrangements of spin orientation is understood as defining the clustering structure of the data.

The Potts model gives a reference to the energy E of the configuration, so that stability requires low energy:

$$\mathcal{H}(s) = -J \sum_{\langle i,j \rangle}^N x_i x_j \quad (1)$$

The transition between the magnetic phases due to variation of temperature can be characterized by the susceptibility χ , a physical parameter that reflects the respective overall magnetization of the system relative to the number of spins with a value between 1 and q , calculated as:

$$\chi = \frac{N}{T} (\langle m^2 \rangle - \langle m \rangle^2) \quad (2)$$

where the variance of magnetization is defined as:

$$m = \frac{(N_{max}/N)q - 1}{q - 1} \quad (3)$$

The lowest energy probabilistic distribution of the system states requires predominance of configurations with similar spins for low temperatures and strong interactions. This distribution is expressed as:

$$P(s) = \frac{1}{Z} \exp\left(\frac{\mathcal{H}(s)}{T}\right) \quad (4)$$

where Z is a normalization constant:

$$Z = \sum_s \exp\left(\frac{-\mathcal{H}(s)}{T}\right) \quad (5)$$

In order to apply these concepts to data sets and optimize the execution of the algorithm, the Swendsen-Wang method was adopted. The motivation of this

approach is to analyse different configurations of the system based on spin neighborhood interactions.

The method proceeds as described in the following. First, we assume a data set containing N variables x_i whose d components are measurements of the system features. In analogy to atoms in a two-dimensional network, we assign a random state s_i among the q possibilities to each respective point x_i .

The ranges and steps of temperature variation are predefined in order to choose the number of interactions in which we want to locate the superparamagnetic behaviour of system. Then, we analyse the probability (4) of connection between the sites with the same spin based on the mutual interaction and neighbourhood criterion. The latter suggests a maximum number K such that the interaction J_{ij} between x_i and x_j is computed only if they are K -nearest neighbors of each other. This interaction is inversely proportional to the average nearest-neighbor distance a and is mathematically defined as:

$$J_{ij} = \frac{1}{K} \exp\left(-\frac{d_{ij}}{2a}\right) \quad (6)$$

By changing the configuration, we estimate the physical parameters of magnetization (3) and the susceptibility (2). This is repeated until the number M of interactions is reached.

The threshold temperatures T_{fs} and T_{ps} , for which the system is in the superparamagnetic phase, can be located by identifying the points of maximal susceptibility and sharp decrease, respectively. In the transition to paramagnetic regime a guess to T_{ps} can be $T = \exp^{1/2} / 4 \ln(1 + \sqrt{q})$.

Aimed at quantifying the ordering properties of the new system configuration, we need to estimate the spin-spin correlation $G_{ij} = \frac{(q-1)\hat{C}_{ij}+1}{q}$, given in Equation 7, which is typically performed by a Monte Carlo procedure.

$$\hat{C}_{ij} = \sum_{\ell=1}^M \frac{I_{ij}(\ell)}{M} \quad (7)$$

where $I_{ij} = 1$ if the points are at the same group or 0 otherwise.

So, it is necessary to identify the Swendsen-Wang groups with connected sites, construct the data clusters, compute the magnetization average $\langle \bar{m} \rangle = \frac{N_{max}}{N}$ and then repeat the above procedure until the maximal range of temperature is reached.

We can verify the different regimes of the superparamagnetic phase through the susceptibility measure. After locating T_{fs} and T_{ps} , we can analyse the superparamagnetic sub-phases assuming their mean temperature $T_{clus} = (T_{fs} + T_{ps})/2$ as the point where the clusters are formed.

The SPC algorithm follows all these steps and concepts, and has many applications. Currently, there are effective and optimized implementations available on the web, such as Tetko's program [21]. We used this software in the current article, described in the next section.

2.4. SPC software

For our data analysis, we used the SPC software implemented by Tetko [21]. It is developed in Java, runs on-line as an applet and is freely available through the VCCLAB (Virtual Computational Chemistry Laboratory) web site at <http://www.vcclab.org/lab/spc>. VCCLAB aims to provide free on-line tools to analyse chemical data [17].

In order to satisfy the required input format, we calculated the Euclidean distance between all data points and saved them in a text file to upload into the SPC program. We used all parameters in the default configuration, since these values are recommended by the author. The output is analysed and discussed in the following section.

3. Results and Discussions

In order to compare the results of SPC and other approaches of morphological analysis, we applied PCA and LDA to the set of neuronal cells, which was selected based in the cell type and brain region. We also verified the agreement between each of the obtained clusters and the original categories.

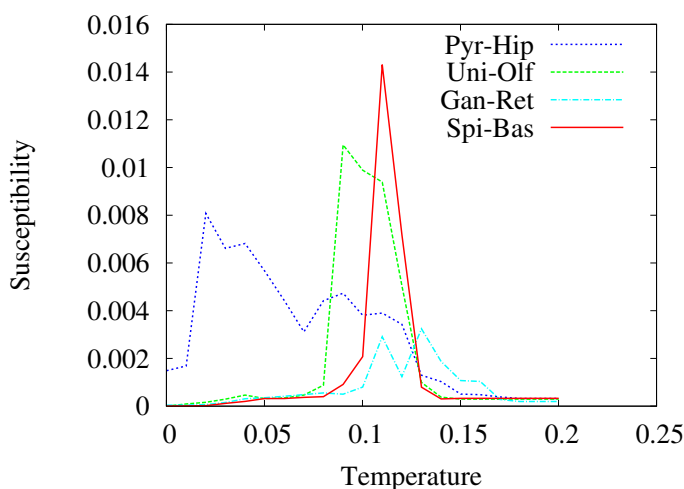


Figure 2. Evolution of the susceptibility parameter to each type-region. Observe the points of maximal and decreasing with which we can identify the superparamagnetic regime.

In both PCA and LDA, the Pyr-Hip cells are scattered, as we can see in Figures 3(a) and 4(a), respectively. This suggests that these neurons exhibit morphological features overlapping the other categories, instead of presenting more homogeneous characteristics which would otherwise imply in their separation from the other groups. The most homogeneous category is the Spi-Bas, which appears as a little, compact region in both methods. The Uni-Olf seems to have a more central position, intermediate to the other clusters. This behaviour is also observed for the Gan-Ret, whose location in LDA shows it to be distinct from the latter category.

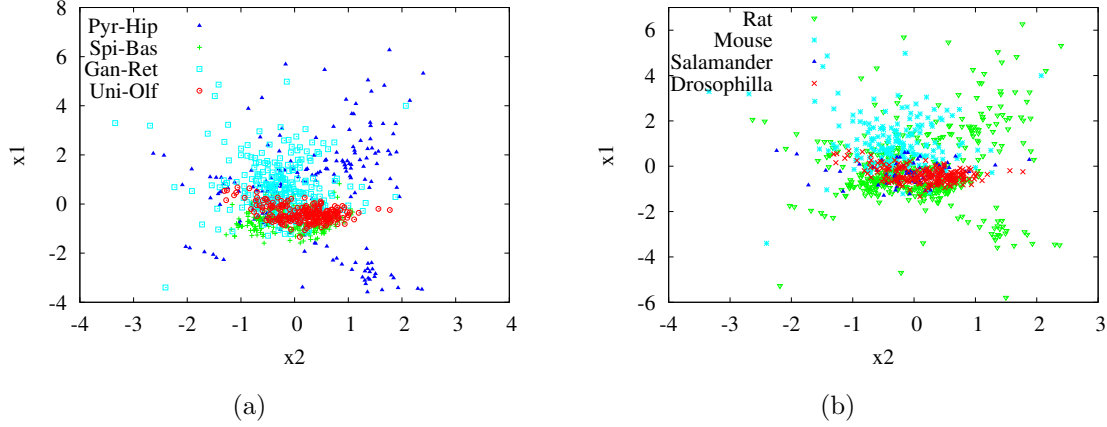


Figure 3. PCA of the four selected cell categories considering the type-region (a) and the species (b) classification. x_1 and x_2 correspond to the first and second components, respectively.

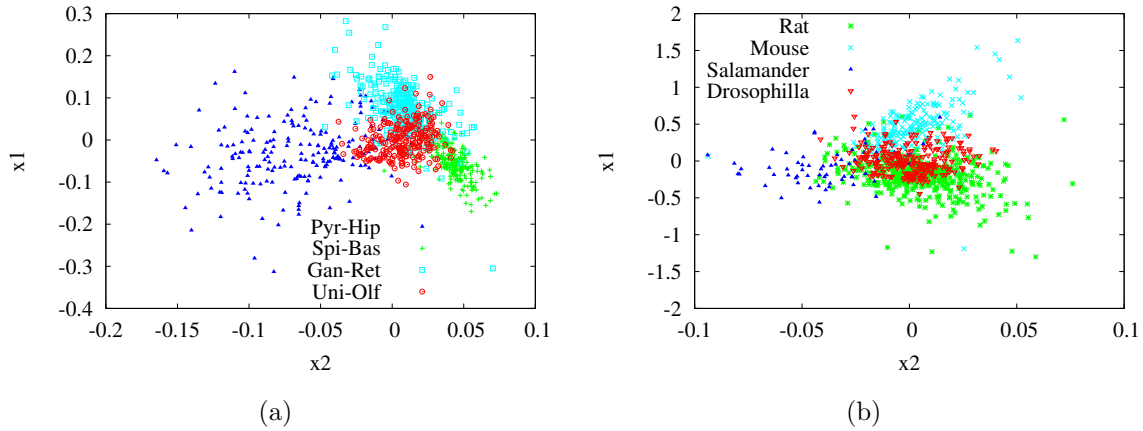


Figure 4. LDA of the four selected cell categories considering the type-region (a) and the species (b) classification. x_1 and x_2 correspond to the first and second components, respectively.

In order to analyse the internal composition of the categories, we applied the SPC method in each one of them and verified the formation of inner clusters by using PCA (Figure 5) and LDA (Figure 6) approaches. The Pyr-Hip category revealed more heterogeneity, splitting in more clusters than the others during the SPC process (five clusters at the mean temperature $T_{clus} = 0.07$). This category also presented a susceptibility curve with a longer superparamagnetic phase, characterizing a behaviour different from those observed for the other classes. On the other hand, the Spi-Bas category presented three clusters not too far from each other and a big and sparse set of non-clustered cases. In the LDA, the homogeneity is indicated by the fact that the respective individuals appeared compacted in a specific region. Regarding the susceptibility curve, its main difference from the other classes is that it has only one peak at the superparamagnetic phase.

In the Gan-Ret category, we observed a single cluster in the superparamagnetic process, and two peaks of susceptibility with approximate values, relatively lower than the peaks on the other classes. The resulting clusters agree with the multivariate methods, especially in a region which overlaps with other categories. We can also see many non-clustered individuals.

The Uni-Olf category presented the most characteristic susceptibility curve, giving rise to two clusters in the obtained distribution. The points are relatively sparse, and a more numerous subcategory can be seen, which is surrounded by many unclassified cases and another small cluster.

Another interesting approach regarding the distribution of the neuronal cells and their categories concerns the investigation about the relationship between type-region and species, as well as the obtained clusters. This study was done for both PCA and LDA (Figures 3(b) and 4(b)) and compared with the direct references of the data set. We identified the species of the selected cells, finding them to correspond to rats, mice, salamanders and drosophillas. So, we count the number of these animals in each category (see Table 1) in order to verify the possible agreement with the results yielded by LDA and PCA. In most part of the measurements, it is possible to verify that the Pyr-Hip category has a significative higher mean value (see Table 2).

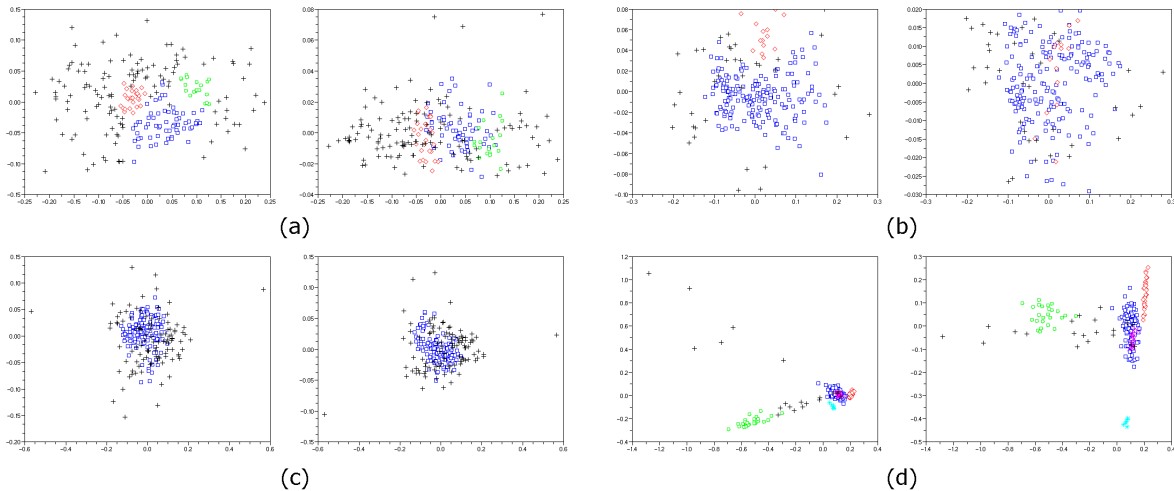


Figure 5. SPC clusters of each category, visualized with PCA: (a) Spi-Bas, (b) Uni-Olf, (c) Gan-Ret, and (d) Pyr-Hip. In each pair of graphics, the left-hand graph shows the components 1 and 2, and the right-hand one exhibits the components 1 and 3.

In order to check about possible influences of the original data properties (e.g. researcher, staining method, etc) on the clusters obtained in the case of the Pyr-Hip cells, we visualized the PCA and LDA multivariate projections marked accordingly to these properties. This category presented five well defined and distinguished clusters that could indicate influence of the original data properties or new distinct subcategories.

The available information about the data is: researcher who provided the data, animal strain, minimum age, maximum age, age scale, gender, minimum weight,

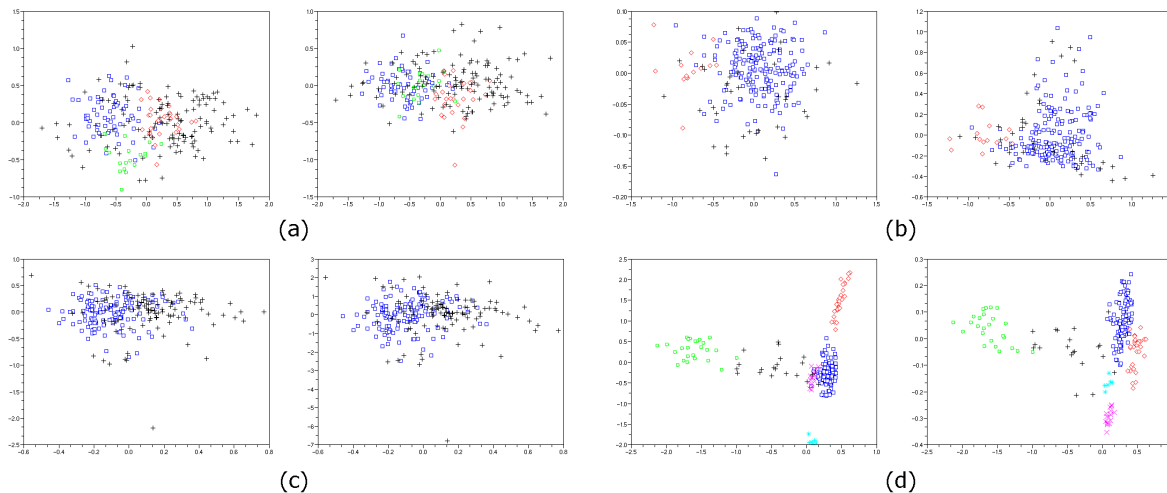


Figure 6. SPC clusters of each category, visualized with LDA: (a) Spi-Bas, (b) Uni-Olf, (c) Gan-Ret, and (d) Pyr-Hip. In each pair of graphics, the left-hand graph shows the components 1 and 2, and the right-hand one exhibits the components 1 and 3.

maximum weight, development, secondary brain region, tertiary brain region, original format, experimenting protocol, staining method, slicing direction, slice thickness, objective type, magnification, reconstruction method, date of deposition and date of upload. In Figure 7, we show only the properties for which we found some relationship with the clusters. The unclustered elements were eliminated and the data was reprojected with LDA, in order to obtain a better visualization of the clusters for this analysis (Figure 7(a)).

Table 3. Pyr-Hip subclusters size.

Cluster	Number of elements
Blue square	111
Red diamond	29
Green square	25
Magenta x	18
Cyan star	6

Table 3 shows the number of elements in the clusters of the Pyr-Hip category. The blue square cluster concentrates more than half of the elements, being underlain by a variety of property classes. On the other hand, the small cyan star cluster always presented its elements stable in the same property class through different information properties, but did not distinguish from the others since its classifications were never exclusive.

The green square cluster is formed by the data from researchers (Figure 7(b)): Larkman (black cross), Barrionuevo (green squares) and part from Turner (red triangles). This cluster did not lead to a unique and concise classification.

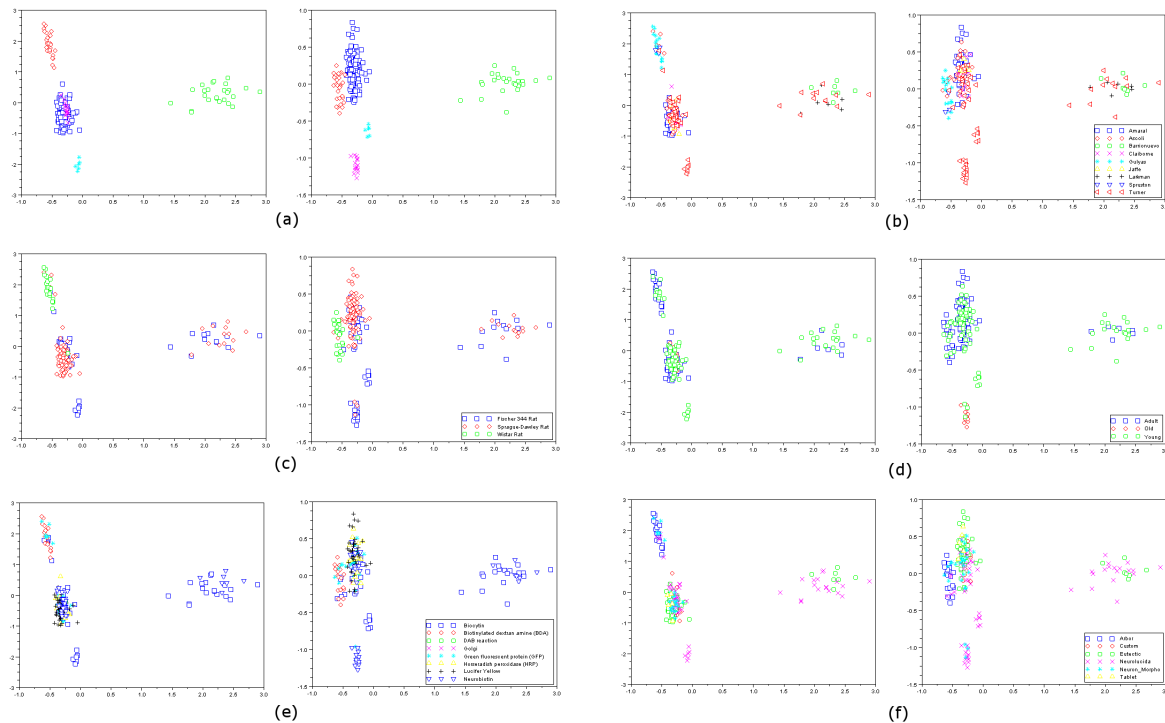


Figure 7. LDA visualization of the clusters found by SPC in the Pyr-Hip category (a), and the original data properties: researcher (b), strain (c), development (d), staining method (e), and reconstruction method (f). In each pair of graphics, the left-hand graph shows the components 1 and 2, and the right-hand one exhibits the components 1 and 3.

The neuronal data produced by the researcher Gulyas constitute almost all elements in the red diamond cluster and has unique classification in the original data properties: staining method (classified as Biotinylated dextran amine - Figure 7(e)) and reconstruction method (classified as Arbor - Figure 7(f)). In the strain category (Figure 7(c)), the Gulyas data shares its classification with the Spruston data. Both are classified as using the strain 'Wistar Rat'. All but one of the four Spruston elements are in the red diamond cluster.

The magenta x cluster comprises all old rats, as we can see in the development data graphic in Figure 7(d). But, it also includes three exceptions (young rats). Examining the data, it was possible to find out that these old rats were 24 months old, while the young exceptions were 1 day old. Thus, although it gets all old rats, there are exceptions at the other side of the age cluster.

Generally, we found no clear correspondence with any of those a priori properties. The fact that the obtained clustering structure could not be clearly explained by the original data properties suggests that the obtained subclusters are a consequence of some intrinsic morphological variation among the considered cells, possibly implying the definition of new categories.

4. Conclusion

Among several challenges in neuroscience, the morphophysiological relationship of the neuronal cells has figured as an enhanced approach in order to establish the characterization and classification of these structures. Currently, the development of these studies have taken advantage of information available in public databases, allowing the application of many pattern recognition and clustering methods. The problem has been continuously investigated, leading to new techniques to classify a data set. The theoretical bases of these procedures can be established in physical real models, as Superparamagnetic Clustering.

Aimed at investigating the clustering structures of the neuronal cells, we extracted many morphological measurements from NeuroMorpho, which is the largest repository currently, and compared the results of multivariate and clustering methods in the most numerous categories, whose analysis was performed considering all category elements and individual categories. In the first case, our purpose was to verify for agreement between the original classification and the categories obtained by the PCA and LDA. Afterwards, we isolated each selected category in order to locate internal clusters and the respective information that could explain their organization. The Pyr-Hip cells seemed to form the most heterogeneous category in both PCA and LDA results, in which remained sparse, as well as in the SPC results, where it had the higher number of clusters. The Gan-Ret category was located as intermediate among other categories and presented two species, despite the result of the SPC that revealed a single cluster surrounded by many unclassified cases. Given that the subclusters obtained for the Pyr-Hip category could not be explained by specific features of the original cells, we understand that they potentially imply in a revision of the current classification in order to account for possible new types of neuronal cells.

New approaches can be used to complete these results, expanding the analysis to more properties, performing correlations and eliminating redundancy between the measurements, as well as the application of other clustering methods, such as the hierarchical Ward method, motivating further studies.

5. Acknowledgments

Mauro Miazaki thanks FAPESP (07/50988-1) for financial support. Luciano da F. Costa is grateful to FAPESP (05/00587-5) and CNPq (301303/06-1) for sponsorship.

References

- [1] E. R. Kandel, J. H. Schwartz, and T. M. Jessel. *Principles of neural science*. McGraw-Hill, New York, 2000.
- [2] T. Trappenberg. *Fundamentals of Computational Neuroscience*. Oxford University Press, USA, 2002.
- [3] R. H. Masland. Neuron cell types. *Curr. Biology*, 14:497–500, 2004.
- [4] Q. Wen and D. B. Chklovskii. A cost-benefit analysis of neuronal morphology. *J. Neurophysiology*, 99:497–500, 2008.
- [5] M. Bota and L. W. Swanson. The neuron classification problem. *Brain Research Reviews*, 56:79–88, 2007.
- [6] S. R. Cajal. *Recollections of my life*. MIT Press, Massachusetts, 1989.
- [7] B. B. Waessle, H. Boycott and R. B. Illing. Morphology and mosaic of on- and off-beta cells in the cat retina and some functional considerations. *The Royal Society*, 212:177–195, 1981.
- [8] H. Waessle and L. Peichl. The structural correlate of the receptive field centre of alpha ganglion cells in the cat retina. *J. Physiology*, 341:309–324, 1983.
- [9] C. R. Hosking and J. L. Schwartz. The future’s bright: Imaging cell biology in the 21st century. *Trends in Cell Biology*, 9(11):553–554, 2009.
- [10] L. da F. Costa. Computer vision based morphometric characterization of neural cells. *Review of Scientific Instruments*, 66:3770–3773, 1995.
- [11] A. E. Dashti, S. Ghandeharizadeh, J. Stone, L. W. Swanson, and R. H. Thompson. Database challenges and solutions in neuroscientific applications. *NeuroImage*, 97:97–115, 1997.
- [12] NeuroMorpho.Org.
- [13] L. da F. Costa and T. J. Velte. Automatic characterization and classification of ganglion cells from salamander retina. *J. Comp. Neurol.*, 404:33–51, 1999.
- [14] J. E. Cook. Getting to grips with neuronal diversity. what is a neuronal type? *Plenum Press*, pages 91–120, 1998.
- [15] J. Stone. *Parallel processing in the visual system: the classification of retinal ganglion cells and its impact on the neurobiology of vision*. Plenum Press, New York, 1983.
- [16] M. Blatt, S. Wiseman, and E. Domany. Superparamagnetic clustering of data. *Physical Review Letters*, 76(18):3251–3254, 1996.
- [17] I. V. Tetko, J. Gasteiger, R. Todeschini, A. Mauri, D. Livingstone, P. Ertl, V. A. Palyulin, E. V. Radchenko, N. S. Zefirov, A. S. Makarenko, V. Y. Tanchuk, and V. V. Prokopenko. Virtual computational chemistry laboratory – design and description. *J. Comput. Aid. Mol. Des.*, 19:453–63, 2005.
- [18] G. A. Ascoli, D. E. Donohue, and M. Halavi. NeuroMorpho.Org: a central resource for neuronal morphologies. *Journal of Neuroscience*, 27(35):9247–9251, 2007.
- [19] M. Halavi, S. Polavaram, D. E. Donohue, G. Hamilton, J. Hoyt, K. P. Smith, and G. A. Ascoli. NeuroMorpho.Org implementation of digital neuroscience: Dense coverage and integration with the NIF. *Journal of Neuroinformatics*, 6(3):241–252, 2008.
- [20] R. Scorcion, S. Polavaram, and G. Ascoli. L-Measure: a web-accessible tool for the analysis, comparison and search of digital reconstructions of neuronal morphologies. *Nature Protocols*, 3:866–76, 2008.
- [21] I. V. Tetko, A. Facius, A. Ruepp, and H.-W. Mewes. Super paramagnetic clustering of protein sequences. *BMC Bioinformatics*, 6:82, 2005.